Published in final edited form as:
PET Clin. 2009 April ; 4(2): 163–172. doi:10.1016/j.cpet.2009.05.001.

PET Imaging of Prostate Cancer Using ^{11}C-Acetate

Johannes Czernin, MD, **Matthias R. Benz, MD**, and **Martin S. Allen-Auerbach, MD**
Department of Molecular and Medical Pharmacology, Ahmanson Biological Imaging Division, David Geffen School of Medicine at the University of California Los Angeles, Los Angeles, CA

Introduction

Tumor metabolic imaging has largely focused on the use of PET imaging with ^{18}F-fluorodeoxyglucose (FDG). This is based on the well-established fact that many cancers are highly glycolytic even in under aerobic conditions [1]. However, some cancers do not consistently exhibit increased FDG uptake. Therefore, the use of imaging other metabolic pathways such as amino acid or lipid metabolism has been explored in cancer [2]. Prostate cancer is one of the entities that exhibits increased glycolysis frequently only in late stages of the disease. On the other hand, several studies have shown that lipid metabolism is increased even in early stages of the disease. The lipogenic phenotype of prostate cancer can be imaged, among others, with ^{11}C-acetate PET.

In the “Cancer Trends Progress Report” of 2007 the National Cancer Institute reported 165 new cases of prostate cancer/100,000 men/year. The life time chance for developing cancer of the prostate is around 15% whereby the cancer risk increases sharply with age.

Early detection of initial and recurrent disease is critical for improving patient outcomes. Prostate cancer is usually detected by serum measurements of Prostate Specific Antigen (PSA) and/or rectal digital examination. Both have a limited sensitivity and specificity [3]. Trans-rectal ultrasound while also used for disease detection is most frequently employed for guiding prostate core biopsies in patients with elevated PSA or abnormal findings on digital rectal examinations. However, this imaging approach is not successful for disease detection if PSA levels are very low (< 0.1 ng/ml).

PET imaging with ^{18}F-fluorodeoxyglucose (FDG) is neither used for prostate cancer screening nor detection. This is because primary prostate cancer does not routinely exhibit a glycolytic phenotype. In addition, small malignant lesions may be below detection limits of PET [4]. Moreover, tracer excretion through the kidney into the bladder obscures the inspection of the prostate bed on FDG-PET images (which could be remedied in part by the use of PET/CT imaging).

Corresponding Author: Johannes Czernin, MD, Professor of Molecular and Medical Pharmacology, Ahmanson Biological Imaging Division; David Geffen School of Medicine at UCLA; 10833 Le Conte Avenue, Los Angeles, CA 90095, Phone: ++1-310-2063226, jczernin@mednet.ucla.edu.

The authors declare no conflicts of interest.

The authors have nothing to disclose.

Tumor recurrence is most frequently established by rising serum PSA levels. If tumor recurrence is confined to the prostate bed localized salvage therapy can be curative. However, if rising PSA levels originate from distant disease, local salvage therapy is no longer an option since it is associated with considerable morbidity without improving survival.

The long term outcome of patients with biochemical recurrence of disease after either prostatectomy or radiation therapy is correlated with pre-salvage therapy serum PSA levels [5, 6]. It is therefore important to detect the site of recurrence as early as possible during the course of relapse. Unfortunately, rising serum PSA levels, the rate of PSA rise (PSA velocity), the interval to PSA relapse and pathological features of the primary tumor do not accurately discriminate between local and distant disease [7, 8].

Metastatic Disease

Advances in diagnostic imaging may result in better selection of patients for adjuvant local versus systemic therapy. The usefulness of computerized tomography (CT) or magnetic resonance imaging (MRI) has recently been investigated prospectively in 375 patients who were at intermediate or high risk for lymph node metastases [9]. For MRI, a novel lymph node specific contrast agent (ferumoxtran-10, consisting of ultra-small particles of iron oxide) was used. These particles migrate from the vascular space into the interstitial space, are taken up by macrophages and are then cleared via lymphatic vessel to finally accumulate in lymph nodes. Because of hemodynamic alterations in the regional lymphatic system induced by metastatic lesions, fewer particle containing macrophages arrive in lymph nodes harboring metastatic disease, which in turn results in different signal intensities on MRI images. Using histology as the gold standard, the specificity of MRI and CT was high at >90%. However, MRI was significantly more sensitive than CT (82 vs. 34%; $p<0.05$). Thus, MRI imaging might play an increasing role for detecting lymph node metastases in patients with evidence of biochemical recurrence.

Metastatic Disease

While MRI is frequently used for initial staging of local lymph node involvement bone involvement is detected by the use of bone scans in patients with PSA levels of > 10 ng/ml. Extensive CT or MRI surveys for distant disease are limited to patients with a high level of suspicion for metastatic disease.

FDG-PET has also been used for detecting metastatic prostate cancer and has a considerable impact on patient management [10–12].

Seltzer et al [13] demonstrated previously that antibody imaging targeting prostate specific membrane antigen (^{111}-indium prostascint) is of limited usefulness for the detection of metastatic prostate cancer. Use of this imaging probe revealed distant disease in only 1/6 patients with known metastases.

Metastatic disease can also be detected with conventional bone scans, ^{18}F-sodium fluoride PET/(CT) bone scans, MRI or CT imaging. None of these techniques alone is well-suited for monitoring therapeutic responses [14].

Current therapeutic options in advanced disease are limited and mainly include hormonal treatments. Several targeted therapeutic approaches are however under investigation but have not yet reached clinical routine [15]. Imaging is unlikely to play a role for detecting primary prostate cancer. However, there is a need to develop imaging approaches that would a) allow for detection of and discrimination between local recurrence and distant metastatic disease, and b) permit the monitoring of tumor responses to novel therapeutic approaches.

Molecular PET imaging probes that have been investigated for these indications include ^{11}C or ^{18}F-choline, ^{18}F-labeled amino acids, antibody approaches and others [16].

This brief review will focus on the potential ability of ^{11}C acetate for improving the care of prostate cancer patients. We will first discuss the biochemical processes that are targeted by ^{11}C acetate imaging, explore its biodistribution and dosimetry and then review the limited data on imaging primary, recurrent and metastatic disease with this metabolic imaging probe.

Biological Correlates of ^{11}C -Acetate Uptake in Prostate Cancer

Major metabolic pathways for acetate include the tricarboxylic cycle [17], as well as lipid and cholesterol synthesis.

^{11}C-acetate is actively transported across cell membranes via mono-carboxylate transporters [18]. After conversion to acetyl CoA in the mitochondria the metabolic fate of ^{11}C-acetate is diverse. In tissues with high rates of oxidative metabolism acetyl CoA enters the TCA cycle resulting in production of carbon-dioxide.

^{11}C-acetate was initially used to measure myocardial oxidative metabolism with external gamma probes [19] or PET [20, 21]. In both approaches the myocardial tracer extraction and clearance kinetics were studied under a variety of conditions (control, ischemia, reperfusion, increased oxygen demand) and ^{11}C-acetate clearance was correlated closely with myocardial oxygen consumption. Externally measured ^{11}C clearance by PET corresponded to CO2 production and thus to tricarboxylic acid cycle activity.

However, increased oxidative metabolism is highly unlikely to account for tumor retention of ^{11}C-acetate. Its retention in prostate cancer is most likely due to increased fatty acid synthesis (Figure 1). Fatty acid synthase (FAS) plays important roles in the de novo synthesis of fatty acids from acetyl-CoA, malonyl-CoA and NADPH in normal and abnormal tissues [22]. Its normal biological functions include the production of lecithin for surfactant, the supply of fatty components of breast milk, and the conversion and storage of energy in liver and adipose tissue. Human cancer cells do not store lipids but rather incorporate them into membranes as phopholipids.

FAS is over-expressed in many human cancers and in particular in prostate cancer [23]. The degree of its over-expression appears to be correlated with tumor aggressiveness [24] and is linked to various oncogenic signal transduction pathways [2]. FAS affects the phospho-lipid content of membrane fractions and participates in controlling the lipid composition of membrane microdomains which might affect signal transduction, cell migration and other processes [25].

Blocking of fatty acid synthase by small interfering RNA (siRNA) or a small molecule inhibitor results in tumor cell death via the caspase 8-mediated apoptotic pathway [17]. It also decreases ^{11}C-acetate uptake in various prostate cancer cell lines [25]. Additional evidence for the critical role of lipid synthesis for maintaining tumor cell proliferation and viability in prostate cancer was provided by Brusselmans et al. who used RNA interference to silence acetyl-CoA-Carboxylase in malignant LNCaP prostate cancer cell lines resulting in growth arrest and apoptosis [26]. Acetyl CoA-Carboxylase is the rate limiting enzyme in the fatty acid synthesis pathway that produces malonyl-CoA. Blocking this enzyme reduces cellular ^{11}C-acetate uptake even more potently than inhibiting FAS (by more than 80%) [27].

Malonyl-CoA is a substrate for fatty acid synthesis and is a negative regulator of fatty acid oxidation. Inhibition of this enzyme with soraphen A, a macrocyclic polyketide, reduced the

phospholipid content of prostate cancer cells and resulted in growth arrest of various prostate cancer cell lines in the G0–G1 cell cycle phase [28]. Importantly, inhibition of the enzyme also resulted in a switch to fatty acid oxidation.

The tumor micro-environment also appears to be a significant determinant of the tumor uptake of ^{11}C-acetate, at least in cell culture. Hara et al [29] provided insights into the relationship between glucose and fatty acid metabolism in human prostate cancer cell lines under normoxic and hypoxic conditions. They examined the uptake of tritiated choline, ^{14}C-acetate and ^{18}F-FDG under normoxic and anoxic conditions in one androgen-independent and another androgen dependent prostate cancer cell line. FDG uptake was highest after 4 hours of anoxia. ^{11}C -acetate uptake was also increased in androgen dependent but not in androgen independent cell lines while choline uptake was reduced in all cell lines under anoxia. Under aerobic conditions choline uptake was higher than that of ^{14}C-acetate which, in turn, was still more than 5 times higher than that of FDG. Androgen depletion resulted in low uptake of all three tracers.

This study confirms several clinical observations: first, FDG imaging might be useful in patients with advanced prostate cancer in whom metastatic lesions are likely to be hypoxic and hence exhibit a glycolytic phenotype; second, ^{11}C-acetate or ^{11}C/^{18}F-choline imaging might be useful for detecting early, “well oxygenated” disease; third, all three probes might be limited in their sensitivity for detecting prostate cancer tissue in patients undergoing anti-androgen treatments. The biochemical alterations underlying these phenotypic changes are well discussed in Hara et al [29].

Biodistribution and Pharmakokinetics of ^{11}C-acetate in Humans

In control rodents, twenty minutes after injection, the pancreas exhibits the highest ^{11}C-acetate uptake. Activity clears from all organs, except the pancreas, within one hour. Tumor ^{11}C-acetate uptake was clearly visible at 30 minutes [30].

Time activity curves obtained from regions of interest placed over serially acquired PET images obtained in a healthy volunteer are shown in Figure 2 [31]. Early tracer uptake in salivary glands, myocardium and kidneys among others is followed by rapid clearance from these tissues. As in rodents and baboons [30], early tracer accumulation is also noted in the pancreas. The normal biodistribution of ^{11}C-acetate in a healthy subject is shown in Figure 3.

At later time points, some bowel activity is noted. The whole body biodistribution of ^{11}C-acetate differs from that of FDG in that its accumulation in the urinary bladder is minimal (Figure 3). Therefore, the prostate bed can be readily inspected on whole body ^{11}C-acetate images.

Tracer kinetics in tumors differ from that in normal tissues such as the myocardium. In tumors, a plateau phase follows flow dependent tracer delivery that is consistent with ^{11}C-acetate retention in tumor cells [32] (Figure 4). In contrast, myocardial time activity curves are characterized by rapid tracer accumulation representing blood flow that is followed by rapid tracer clearance when acetate is metabolized in the TCA cycle. More than 80% of C-11 acetate is cleared after 20 minutes.

These discrepant time activity curves between tumor and heart strongly suggest that the retention of ^{11}C-acetate in tumor tissue is largely unrelated to TCA cycle activity and is accounted for by incorporation of acetate into the lipid pool.

In summary, the degree to which various lipid metabolic pathways and their individual steps contribute to the retention of ^{11}C-acetate in prostate cancer tissue are incompletely understood. However, it appears that incorporation into the lipid pool, and more specifically into membrane lipids [33] largely accounts for the preferential retention of ^{11}C-acetate in prostate cancer while fatty acid oxidation plays a only a limited role, if any at all.

Clinical studies Using C-11 Acetate

^{11}C-Acetate Dosimetry

The organ dosimetry has been established [31] from studies in 6 healthy volunteers who underwent serial whole body PET imaging after the intravenous injection of 525 MBq (14.2 mCi) of ^{11}C acetate. The organs receiving the highest doses were the pancreas (critical organ receiving 0.017 mGy/MBq), bowel, kidneys and spleen.

Clinical Imaging protocols

Because of the short half life of ^{11}C-acetate imaging commences from 2–10 minutes after tracer injection. Injected doses range from 555–1110 MBq (15–30 mCi). In patients with suspected recurrence images of the pelvis are acquired first. Imaging times per bed position range from 5–10 minutes to achieve adequate activity count rates. Depending upon the clinical question to be addressed the imaging field is subsequently expanded to include the abdomen and, if needed, the chest.

When PET/CT is used, a CT scan with or without intravenous contrast is acquired first. This is used both for attenuation correction and as a diagnostic CT study. The extent of the imaging field depends upon the clinical question asked, the patient stage and the individual patient risk profile for distant metastatic disease.

Detection of Prostate Cancer

One of the first questions to be addressed in clinical studies is whether the degree of ^{11}C-acetate permits to differentiate normal prostate tissue from benign hyperplasia and prostate cancer. Using a conventional PET scanner, Kato et al [34] demonstrated in 36 research volunteers that the degree of ^{11}C-acetate uptake was comparable among 6 patients with prostate cancer, 21 volunteers without prostate pathology and nine individuals with benign prostate hyperplasia. Furthermore, the authors showed that the normal prostate shows increasing ^{11}C-acetate uptake with age. Both findings demonstrate that ^{11}C -acetate uptake is not specific for prostate cancer and not well-suited as a screening tool.

In one study of 22 patients with recently diagnosed disease ^{11}C-acetate PET detected prostate cancer with a higher sensitivity than FDG. The standardized uptake value (SUV) of ^{11}C-acetate as measured at approximately 20 minutes after tracer injection ranged from 3.2 to 9.9 (which was significantly higher than the FDG SUV). Since all patients had known prostate cancer, the specificity of the test could not be examined in this study.

In summary, the available literature on primary prostate cancer detection with ^{11}C-acetate is very limited. However, it suggests that ^{11}C-acetate cannot be proposed for prostate cancer screening (because of the comparable tracer uptake levels among cancer, hyperplasia and even normal prostate tissue). Nevertheless, the data demonstrate that ^{11}C-acetate uptake is “visible” and measurable by means of SUV in prostate tissue. This is important because the most interesting potential application of ^{11}C-acetate imaging is the detection of prostate cancer recurrence. For this indication the issue of specificity is clinically much less relevant.

Recurrent and Metastatic Prostate Cancer

Biochemical evidence of prostate cancer recurrence after radical prostatectomy or radiation treatment, frequently defined as a serum PSA level of 0.2 ng/ml, precedes the clinical manifestations of recurrent disease. Once metastatic disease develops the prognosis is poor with an overall patient survival of 5 years [35]. In patients with locally recurrent disease salvage radiation therapy can improve patient survival [6]. The main diagnostic challenge is therefore to detect and localize early cancer recurrence. Several studies evaluated the relationship between serum PSA levels and detection of prostate cancer recurrence with ^{11}C-acetate PET. In one study of 25 patients, the degree of ^{11}C-acetate uptake (SUV) correlated with serum PSA levels [36].

In an early trial [37] of patients with suspected recurrence (based on serum PSA measurements) trans-rectal ultrasound followed by biopsy served as gold standard for ^{11}C-acetate imaging findings. PET was true positive for disease recurrence in 15/18 patients with biopsy proven recurrence and true negative in all 13 patients without recurrent disease (sensitivity and specificity of 83 and 100%, respectively). In this study PET was positive in 4 of 5 patients with biopsy proven cancers and serum PSA levels of <2 ng/ml.

A reasonable detectability of disease in patients with low PSA levels was recently also reported by Albrecht et al. [38]. In their study 17 patients were imaged after primary radiation therapy and 15 after radical surgery. All had biochemical evidence for recurrent disease. PSA levels were significantly higher after radiation treatment (6 ng/ml) than after radical prostatectomy (0.4ng/ml). PET and non-contrast enhanced CT images were fused using a commercially available fusion software. An arbitrary SUV threshold of 2.0 was selected for discriminating between equivocal and positive PET results. In the 17 post-radiation therapy patients, PET suggested local recurrences in 14 patients and was true positive in 5/6 patients with positive biopsy. The detection of bone metastases with ^{11}C-acetate was, however, limited when bone scans and CT were used as reference standards. Recurrence by ^{11}C-acetate was suggested in 9/15 patients who underwent primary surgery and PET was similarly sensitive (approximately 60%) in patients with serum PSA levels of less than 0.8 ng/ml.

In contrast, a poor detection of recurrent disease in patients with low serum PSA levels was reported by the St. Louis group who used ^{11}C-acetate and ^{18}F-FDG PET imaging in 46 patients [39]. Their study group included patients who had undergone radiation and others who underwent surgery as primary treatment. A variety of clinical studies including bone scans, CT scans, biopsy and others served as reference standard for the PET findings. As a physiological variant, the authors noted frequent mild ^{11}C-acetate in inguinal lymph nodes (not reported elsewhere) and considered this a normal pattern. ^{11}C- acetate images suggested with intermediate or high probability the presence of disease in 59% of the patients while FDG-PET imaging suggested disease in only 17% of the participants. It is noteworthy that ^{11}C acetate PET was positive in 59% of patients with PSA levels of >3ng/ml but only in 4% of those with serum levels <3 ng/ml. Based on extensive clinical experience Reske et al suggested that PET/CT imaging or fused PET and MRI images allow for better detection of local recurrence [40]. This notion is supported by the results of a small pilot trial that employed ^{11}C-acetate PET/CT in 11 patients with serum PSA levels of <0.3 ng/ml. The authors identified the site of recurrence in 6/11 patients [41].

However, even with PET/CT the site of recurrence might be difficult to identify in patients with low serum PSA levels. In one study software fusion of CT or MRI and PET images in 50 patients with biochemical evidence for recurrent disease [42] resulted in markedly improved accuracy for disease detection and localization. Image fusion changed interpretation from equivocal to normal in 10% and from equivocal to abnormal in 18% of

the lesions. Patient management was affected in 28% of the patients. A gold standard (biopsy) for verification of PET findings was only available in a small subset of patients. In general, patients with false negative PET findings had low serum PSA values (median 0.9 ng/ml). However, the authors correctly noted that in four of the six patients with a PSA ranging from to 2.6 – 13 ng/mL after radical prostatectomy, the ^{11}C-acetate scan was also false negative.

Using ^{11}C -acetate PET/(CT), Sandblom et al [43] enrolled 20 patients with elevated PSA levels that ranged from 0.5 to 8.1 ng/ml after radical prostatecotmy. All underwent ^{11}C-acetate PET/CT imaging (Figure 5) in addition to all standard examinations performed for identifying cancer recurrence sites. ^{11}C-acetate identified disease sites in 75% of the patients. All PET positive patients had serum PSA levels of greater than 2.0 ng/ml and SUVs ranged from 2.0 to 8.1 in these patients. “False positive” findings occurred in 3 patients. One exhibited tracer uptake in the chest which was subsequently confirmed to represent non-small cell lung cancer, while two other patients had inflammatory changes, one in the esophagus and the other one in the mediastinum. This confirms that ^{11}C-acetate uptake is not cancer specific but rather a probe of lipid metabolism which can also be altered in inflammatory disease.

In summary recurrent prostate cancer can be detected with ^{11}C-acetate but since detectability appears to be correlated with serum PSA levels, detectability is limited in patients with serum PSA levels below 3 ng/ml.

Comparative Studies

Several groups have compared the diagnostic performance of ^{11}C acetate with that of other metabolic PET imaging probes in patients with prostate cancer. In a small pilot trial of 12 patients with prostate cancer [44] the biodistribution of ^{11}C-acetate and ^{11}C-choline, a substrate of choline kinase that is also incorporated into membrane lipids, was compared in patients after initial diagnosis, at the time of biochemical recurrence or after radical prostatectomy. ^{11}C-acetate uptake was high in spleen and pancreas whereas ^{11}C-choline uptake was most prominent in liver and kidneys. Importantly, ^{11}C-acetate was not excreted into the bladder while urinary excretion was variable for ^{11}C-choline. With regards to tumor uptake both imaging probes missed small prostatic lesions and 3/13 small metastatic lymph nodes that were confirmed by surgery/pathology. Thus, the diagnostic performance of both imaging probes was comparable.

Another comparison between these probes was conducted by Vees et al in 20 patients [41]. However, the study design differed in that 10 patients were imaged with ^{11}C-choline while the remaining 10 were studied with ^{11}C -acetate. Both tracers provided a comparable cancer detection rate with abnormal local tracer uptake in five/10 patients with ^{11}C-choline and 6/10 with ^{11}C -acetate. The authors concluded that both tracers detect about 50% of cancer recurrences but that endorectal MRI, which detected 15 of 18 recurrences, was superior.

Fricke et al [36] compared lesion detectability using ^{18}F-FDG and ^{11}C-acetate imaging in a small, heterogeneous population of prostate cancer patients that included patients with primary cancer, those with suspected relapse and some with metastatic disease. Overall sensitivity of the acetate approach was 83% which was slightly better than that for FDG (75%). Local recurrence was better detected with^{11}C-acetate while distant disease was better visualized with ^{18}F-FDG.

Taken together these studies suggest that ^{11}C/^{18}F choline and ^{11}C-acetate appear to have a comparable accuracy for detecting local recurrence while FDG PET might be better suited for detecting metastatic disease.

^{18}F-fluoroacetate: Owing to its short half-life of 20.4 minutes the use of ^{11}C-labeled PET imaging probes requires an on-site cyclotron. With this limitation in mind the Washington University group synthesized ^{18}F-fluoroacetate and studied its biodistribution in mice and baboons using a small animal PET system and a human scanner [30]. While defluorination occurred in rodents, this was not observed in baboons. However, the biodistribution of ^{11}C- and ^{18}F-acetate differed. For instance, ^{11}C-acetate blood activity was lower than that of the fluorinated analogue. On the other hand, tumor uptake of ^{18}F acetate was 5 times higher that than of ^{11}C-acetate 30 minutes after intravenous injection. ^{18}F-fluoroacetate tumor to background ratios (other than blood) from various tissues were consistently higher than those for ^{11}C-acetate. Thus, this probe shows promise for imaging prostate and other cancers that exhibit low FDG uptake.

Summary

^{11}C-acetate can be used to image prostate cancer and in particular recurrent disease. Limitations include its low sensitivity for disease detection at low serum PSA levels. The routine use of PET/CT imaging will further improve the diagnostic accuracy of this approach.

Importantly, novel therapeutic approaches targeting tumor lipid metabolism are under development [45]. It is conceivable that imaging of tumor lipid metabolism with ^{11}C/^{18}F-acetate could provide a valuable readout for assessing drug effects on the lipogenic phenotype in vivo.

References

1. Warburg O, Posener K, Negelein E VIII. The metabolism of cancer cells. Biochem Zeitschr. 1924; 152:129–169.
2. Plathow C, Weber W. Tumor Cell Metabolism Imaging. J Nucl Med. 2008; 49(suppl 2):43S–63S. [PubMed: 18523065]
3. Crupp M, Oesterling J. Prostate-specific antigen, digital rectal examination, and transrectal ultrasonography: their roles in diagnosing early prostate cancer. Mayo Clin Proc. 1993; 68:297–306. [PubMed: 7682639]
4. Hofer C, Laubenbacher C, Block T, Breul J, Hartung R, Schwaiger M. Fluorine-18-Fluorodeoxyglucose Positron Emission Tomography Is Useless for the Detection of Local Recurrence after Radical Prostatectomy. Eur Urol. 1999; 36:31–35. [PubMed: 10364652]
5. Cox J, Gallagher M, Hammond E, Kaplan R, Schellhammer P. Consensus statements on radiation therapy of prostate cancer: guidelines for prostate re-biopsy after radiation and for radiation therapy with rising prostate-specific antigen levels after radical prostatectomy. American Society for Therapeutic Radiology and Oncology Consensus PAnel. J Clin Oncol. 1999; 17:1155–1163. [PubMed: 10561174]
6. Stephenson AJ, Shariat SF, Zelefsky MJ, et al. Salvage radiotherapy for recurrent prostate cancer after radical prostatectomy. Jama. Mar 17; 2004 291(11):1325–1332. [PubMed: 15026399]
7. Leibman B, Dillioglugil O, Wheeler T, Scardino P. Distant metastasis after radical prostatectomy in patients without an elevated serum prostate specific antigen level. Cancer. 1995; 76:2530–2534. [PubMed: 8625081]
8. Partin A, Oesterling J. The clinical usefulness of prostate specific antigen: update 1994. J Urol. 1994; 152:1358–1368. [PubMed: 7523702]
9. Heesakkers RAM, Hövels AM, Jager GJ, et al. MRI with a lymph-node-specific contrast agent as an alternative to CT scan and lymph-node dissection in patients with prostate cancer: a prospective multicohort study. The Lancet Oncology. 2008; 9(9):850–856. [PubMed: 18708295]
10. Hillner B, Siegel B, Shields A, et al. The impact of positron emission tomography (PET) on expected management during cancer treatment: Findings of the National Oncologic PET Registry. Cancer. 2009; 115:410–418. [PubMed: 19016303]

11. Hillner BE, Liu D, Coleman RE, et al. The National Oncologic PET Registry (NOPR): design and analysis plan. J Nucl Med. Nov; 2007 48(11):1901–1908. [PubMed: 17942807]
12. Hillner BE, Siegel BA, Liu D, et al. Impact of positron emission tomography/computed tomography and positron emission tomography (PET) alone on expected management of patients with cancer: initial results from the National Oncologic PET Registry. J Clin Oncol. May 1; 2008 26(13):2155–2161. [PubMed: 18362365]
13. Seltzer M, Barbaric Z, Belldegrun A, et al. Comparison of helical computerized tomography, positron emission tomography and monoclonal antibody scans for evaluation of lymph node metastases in patients with prostate specific antigen relapse after treatment for localized prostate cancer. Journal of Urology. 1999; 162:1322–1328. [PubMed: 10492189]
14. Israel O, Goldberg A, Nachtigal A, et al. FDG-PET and CT patterns of bone metastases and their relationship to previously administered anti-cancer therapy. European Journal of Nuclear Medicine and Molecular Imaging. 2006; 33(11):1280–1284. [PubMed: 16791597]
15. Chen Y, Sawyers C, Scher H. Targeting the androgen receptor pathway in prostate cancer. Current Opinion in Pharmacology. 2008; 8(4):440–448. [PubMed: 18674639]
16. Larson S, Schöder H. Advances in positron emission tomography applications for urologic cancers. Current Opinion in Urology. 2008; 18:65–70. [PubMed: 18090493]
17. Knowles LM, Yang C, Osterman A, Smith JW. Inhibition of fatty-acid synthase induces caspase-8-mediated tumor cell apoptosis by up-regulating DDIT4. J Biol Chem. Nov 14; 2008 283(46): 31378–31384. [PubMed: 18796435]
18. Waniewski RA, Martin DL. Preferential utilization of acetate by astrocytes is attributable to transport. J Neurosci. Jul 15; 1998 18(14):5225–5233. [PubMed: 9651205]
19. Brown M, Marshall DR, Sobel BE, Bergmann SR. Delineation of myocardial oxygen utilization with carbon-11-labeled acetate. Circulation. Sep; 1987 76(3):687–696. [PubMed: 3113765]
20. Buxton D, Nienaber C, Luxen A, et al. Noninvasive quantitation of regional myocardial oxygen consumption in vivo with [1–11C]acetate and dynamic positron emission tomography. Circulation. 1989; 79:134–142. [PubMed: 2783396]
21. Buxton DB, Schwaiger M, Nguyen A, Phelps ME, Schelbert HR. Radiolabeled acetate as a tracer of myocardial tricarboxylic acid cycle flux. Circ Res. Sep; 1988 63(3):628–634. [PubMed: 3136951]
22. Kuhajda FP. Fatty Acid Synthase and Cancer: New Application of an Old Pathway. Cancer Res. 2006; 66:5977–5980. [PubMed: 16778164]
23. Baron A, Migita T, Tang D, Loda M. Fatty acid synthase: A metabolic oncogene in prostate cancer? Journal of Cellular Biochemistry. 2003; 91:47–53. [PubMed: 14689581]
24. Epstein J, Carmichael M, Partin A. OA-519 (fatty acid synthase) as an independent predictor of pathologic state in adenocarcinoma of the prostate. Urology. 1995; 45:81–86. [PubMed: 7817483]
25. Swinnen J, Van Veldhoven P, Timmermans L, et al. Fatty acid synthase drives the synthesis of phospholipids partitioning into detergent-resistant membrane microdomains. Biochemical and Biophysical Research Communications. 2003; 302(4):898–903. [PubMed: 12646257]
26. Brusselmans K, De Schrijver E, Verhoeven G, Swinnen J. RNA interference-mediated silencing of the acetyl-CoA-carboxylase-alpha gene induces growth inhibition and apoptosis of prostate cancer cells. Cancer Res. 2005; 65:6719–6725. [PubMed: 16061653]
27. Vavere A, Kridel S, Wheeler F, Lewis J. 1–11C-Acetate as a PET Radiopharmaceutical for Imaging Fatty Acid Synthase Expression in Prostate Cancer. J Nucl Med. 2008; 49:327–334. [PubMed: 18199615]
28. Beckers A, Organe S, Timmermans L, et al. Chemical Inhibition of Acetyl-CoA Carboxylase Induces Growth Arrest and Cytotoxicity Selectively in Cancer Cells. Cancer Research. 2007; 67:8180–8187. [PubMed: 17804731]
29. Hara T, Bansal A, DeGrado T. Effect of hypoxia on the uptake of [methyl-3H]choline, [1–14C] acetate and [18F]FDG in cultured prostate cancer cells. Nuclear Medicine and Biology. 2006; 33(8):977–984. [PubMed: 17127170]
30. Ponde D, Dence C, Oyama N, et al. 18F-Fluoroacetate: A Potential Acetate Analog for Prostate Tumor Imaging—In Vivo Evaluation of 18F-Fluoroacetate Versus 11C-Acetate. J Nucl Med. 2007; 48:420–428. [PubMed: 17332620]

31. Seltzer M, Jahan S, Sparks R, et al. Radiation Dose Estimates in Humans for 11C-Acetate Whole-Body PET. J Nucl Med. 2004; 45:1233–1236. [PubMed: 15235071]
32. Schiepers C, Hoh CK, Nuyts J, et al. 1–11C-acetate kinetics of prostate cancer. J Nucl Med. Feb; 2008 49(2):206–215. [PubMed: 18199613]
33. Yoshimoto M, Waki A, Yonekura Y, et al. Characterization of acetate metabolism in tumor cells in relation to cell proliferation: acetate metabolism in tumor cells. Nucl Med Biol. Feb; 2001 28(2): 117–122. [PubMed: 11295421]
34. Kato T, Tsukamoto E, Kuge Y, et al. Accumulation of [11C]acetate in normal prostate and benign prostatic hyperplasia: comparison with prostate cancer. European Journal of Nuclear Medicine and Molecular Imaging. 2002; 29(11):1492–1495. [PubMed: 12397469]
35. Pound C, Partin A, Eisenberger M, Chan D, Pearson J, Walsh P. Natural History of Progression After PSA Elevation Following Radical Prostatectomy. JAMA. 1999; 281:1591–1597. [PubMed: 10235151]
36. Fricke E, Machtens S, Hofmann M, et al. Positron emission tomography with 11C-acetate and 18F-FDG in prostate cancer patients. European Journal of Nuclear Medicine and Molecular Imaging. 2003; 30(4):607–611. [PubMed: 12589476]
37. Kotzerke J, Volkmer B, Neumaier B, Gschwend J, Hautmann R, Reske S. Carbon-11 acetate positron emission tomography can detect local recurrence of prostate cancer. European Journal of Nuclear Medicine and Molecular Imaging. 2002; 29(10):1380–1384. [PubMed: 12271422]
38. Albrecht S, Buchegger F, Soloviev D, et al. 11C-acetate PET in the early evaluation of prostate cancer recurrence. European Journal of Nuclear Medicine and Molecular Imaging. 2007; 34(2): 185–196. [PubMed: 16832632]
39. Oyama N, Miller T, Dehdashti F, et al. 11C-acetate PET imaging of prostate cancer: detection of recurrent disease at PSA relapse. J Nucl Med. 2003; 44:549–555. [PubMed: 12679398]
40. Reske S, Blumstein N, Glatting G. PET und PET/CT in der Rezidivdiagnostik des Prostatakarzinoms. Der Urologe A. 2006; 45(10):1240–1250.
41. Vees H, Buchegger F, Albrecht S, et al. 18F-choline and/or 11C-acetate positron emission tomography: detection of residual or progressive subclinical disease at very low prostate-specific antigen values (<1 ng/mL) after radical prostatectomy. BJU International. 2007; 99:1415–1420. [PubMed: 17428249]
42. Wachter S, Sandra T, Kurtaran A, et al. 11C-Acetate Positron Emission Tomography Imaging and Image Fusion With Computed Tomography and Magnetic Resonance Imaging in Patients With Recurrent Prostate Cancer. J Clin Oncol. 2006; 24:2513–2519. [PubMed: 16636343]
43. Sandblom G, Sörensen J, Lundin N, Häggman M, Malmström P. Positron emission tomography with c11-acetate for tumor detection and localization in patients with prostate-specific antigen relapse after radical prostatectomy. Urology. 2006; 67(5):996–1000. [PubMed: 16698359]
44. Kotzerke J, Volkmer B, Glatting G, et al. Intraindividual comparison of [11 C]acetate and [11 C]choline PET for detection of metastases of prostate cancer. Nuklearmedizin. 2003; 42:25–30. [PubMed: 12601451]
45. Zhou W, Han W, Landree L. Fatty acid synthase inhibition activates AMP-activated protein kinase in SKOV3 human ovarian cancer cells. Cancer Res. 2007; 67:2964–2971. [PubMed: 17409402]

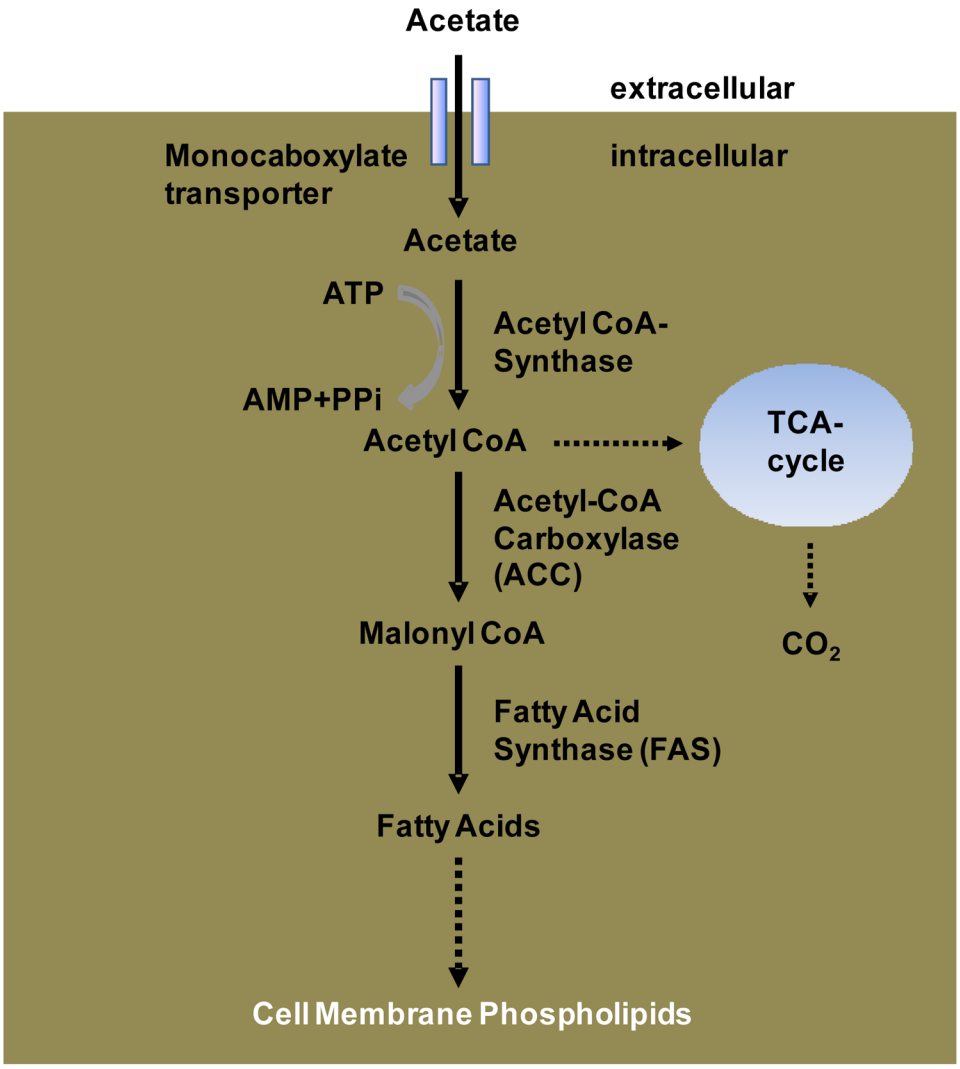

Figure 1.
Simplified Schematic of Fatty Acid Synthesis: Fatty Acid Synthase (FAS) catalyses the de-novo synthesis of fatty acid from Actetyl-CoA, Malonyl-CoA and NADPH. Following several reactions and modifications fatty acids are incorporated into membranes as phospholipids.

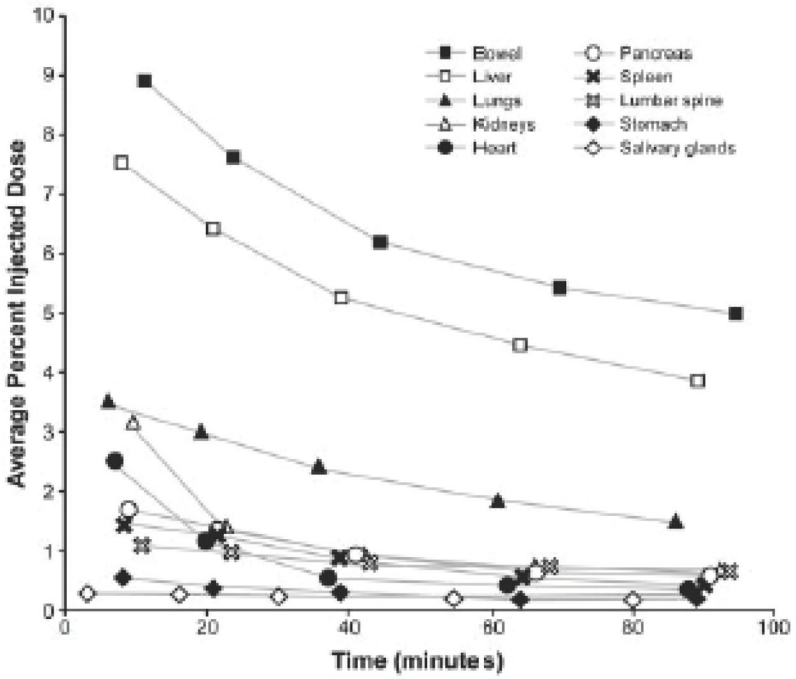

Figure 2.

Tissue time activity curves obtained from serial ^{11}C-acetate images obtained in healthy subjects. Note that activity in pancreas and liver remains relatively high at 100 minutes after tracer injection (Reprinted with permission from reference 31).

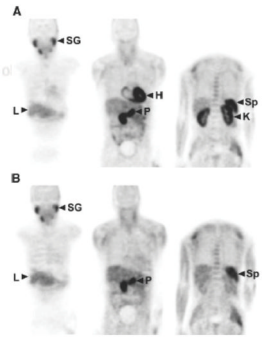

Figure 3.
Normal biodistribution of ^{11}C-acetate in a healthy subject. Images in the upper row (A) were obtained 2 minutes after tracer injection while those at the bottom (B) were acquired 28 minutes after injection of C-11 acetate. L=liver; H=heart; P=Pancreas; Sp= Spleen; SG=Salivary Glands; K=Kidneys; (Reprinted with permission from Reference 31).

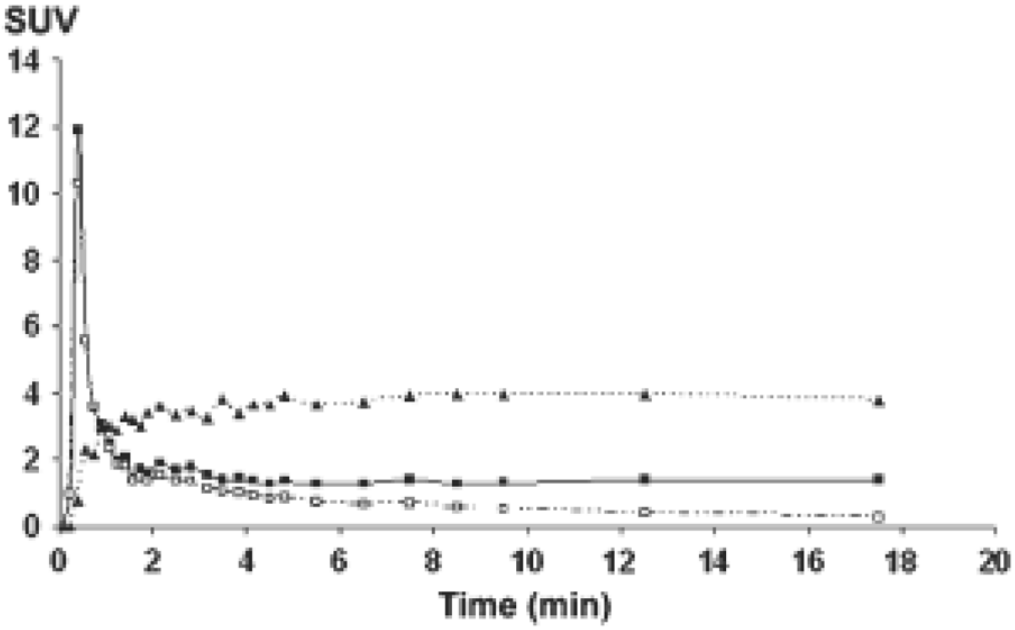

Figure 4.

Time–activity-curves from iliac arteries (squares, solid line), metabolite-corrected input function (open squares, dashed line), and prostate tumor (triangles, dotted line). Uptake is expressed in SUV (standardized uptake value). Data obtained in a 65-y-old man with primary prostate cancer. Note the relative stable activity of ^{11}C-acetate in prostate cancer tissue during the first 20 minutes after tracer injection. (Reprinted with permission from reference 32).

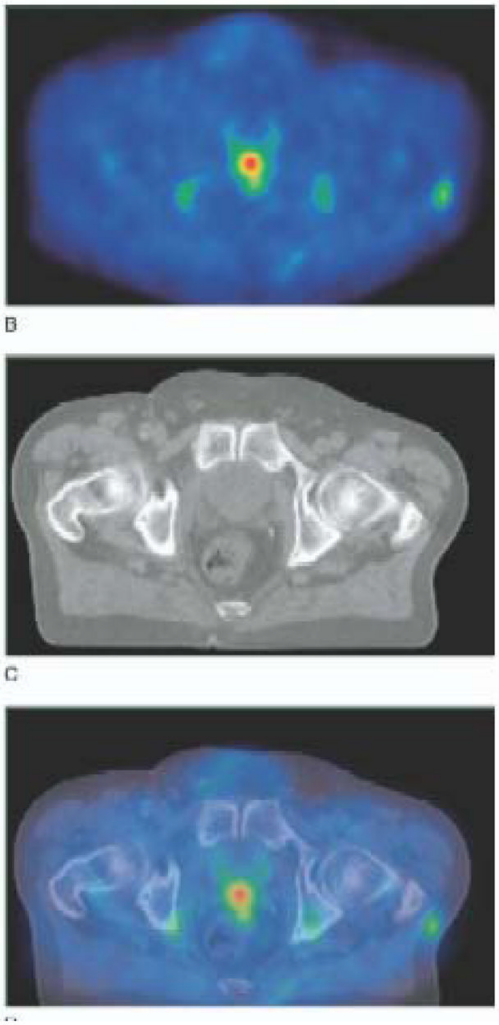

Figure 5.
^{11}C-acetate PET (A), non contrast enhanced CT (B) and fused PET/CT images (C) in a patient with biochemical recurrence and a serum PSA level of 2.5 ng/ml. The SUVmax of the lesion in the prostate bed was 5. Note the absence of tracer accumulation in the urinary bladder (Reprinted with permission from reference 43).